

Raman scattering and electrical resistance of highly disordered graphene

I. Shlimak,^{1,*} A. Haran,² E. Zion,³ T. Havdala,³ Yu. Kaganovskii,¹ A. V. Butenko,³ L. Wolfson,¹ V. Richter,⁴ D. Naveh,² A. Sharoni,³ E. Kogan,¹ and M. Kaveh¹

¹*Jack and Pearl Resnick Institute, Department of Physics, Bar-Ilan University, Ramat-Gan 52900, Israel*

²*Faculty of Engineering, Bar-Ilan University, Ramat-Gan 52900, Israel*

³*Department of Physics and Institute of Nanotechnology and Advanced Materials, Bar-Ilan University, Ramat-Gan 52900, Israel*

⁴*Solid State Institute and Physics Department, Technion-Israel Institute of Technology, Haifa 32000, Israel*

(Dated: December 7, 2024)

Raman scattering (RS) spectra and current-voltage characteristics at room temperature were measured in six series of small samples fabricated by means of electron-beam lithography on the surface of a large size (5x5 mm) industrial monolayer graphene film. Samples were irradiated by different doses of C^+ ion beam up to 10^{15} cm^{-2} . It was observed that at the utmost degree of disorder, the Raman spectra lines disappear which is accompanied by the exponential increase of resistance and change in the current-voltage characteristics. These effects are explained by suggestion that highly disordered graphene film ceases to be a continuous and splits into separate fragments. The relationship between structure (intensity of RS lines) and sample resistance is defined. It is shown that the maximal resistance of the continuous film is of order of reciprocal value of the minimal graphene conductivity $\pi h/4e^2 \approx 20 \text{ kOhm}$.

PACS numbers: 73.22.Pr

I. INTRODUCTION

In recent years, disordered graphene attracts the attention of many researchers¹⁻³. Mainly, this is due to the possibility of obtaining a high-resistance state of graphene films, which is of interest for application in electronics. In the experiment, the disorder is achieved in various ways: by oxidation⁴, hydrogenation⁵, chemical doping⁶, irradiation by different ions with different energies⁷⁻¹¹. In this work the ion bombardment technique is used to gradually induce disorder in graphene. To probe the evolution of disorder, the Raman spectroscopy and resistance measurements are used.

The main new results of this work consist in (i) observation of the utmost degree of disorder induced by ion irradiation, when graphene, due to high density of defects, is no longer continuous film but split into separate fragments. This leads to complete disappearance of the Raman scattering spectra (RS) and change in the mechanism of electrical conductivity; (ii) determination of a correlation between intensity of RS lines and sample resistance in disordered graphene films: transition from the low-defect density regime to the high-defect density regime in RS occurs at the resistance equal to reciprocal value of the minimal graphene conductivity $\pi h/4e^2 \approx 20 \text{ kOhm}$.

II. SAMPLES

The initial specimens were purchased in "Graphenea" company. Monolayer graphene was produced by CVD on copper catalyst and transferred to a 300 nm SiO_2/Si substrate using wet transfer process. The specimen size was $5 \times 5 \text{ mm}$. Graphene film of such a large size was not a monocrystalline. It looks like a polycrystalline film

with the average size of microcrystals about few microns (Fig. 1).

On one of these specimens, gold electrical contacts were deposited directly on the graphene surface through a metallic mask. This sample is marked as "0". On the other 5x5 mm specimen, many samples of small size ($200 \times 200 \mu\text{m}$) as well as electrical contacts (5 nm Ti and 45 nm Pd) thereto were made using electron beam lithography (EBL). Optical observation and electrical testing after EBL showed that some of small samples are damaged, the total yield was about 65%. This reduced yield can be explained by the influence of the triple lift-off process in the case of large size polycrystalline graphene film. One can assume that the boundary between single crystals is a weakness which can be damaged during the lift-off process. For further measurements, only intact samples were selected.

All small samples on the surface of the common 5x5 mm specimen were grouped into 6 groups. The first group was not irradiated. Samples from this group have a mark "1". Groups "2-6" were irradiated by C^+ ions with energy 35 keV at five different doses: 5×10^{13} , 1×10^{14} , 2×10^{14} , 4×10^{14} and $1 \times 10^{15} \text{ cm}^{-2}$ correspondingly. Samples from these groups have marks from 2 to 6. Below, we report the results of measurements of the RS spectra and two-probes electrical resistance in these samples at room temperature

III. RAMAN SCATTERING

In the RS spectra measurements, excitation was realized by the laser beam with $\lambda = 532 \text{ nm}$ and power less than 2 mW to avoid heating and film destruction. Reproducibility was verified by repeated measurements in the same point and in different samples of the same

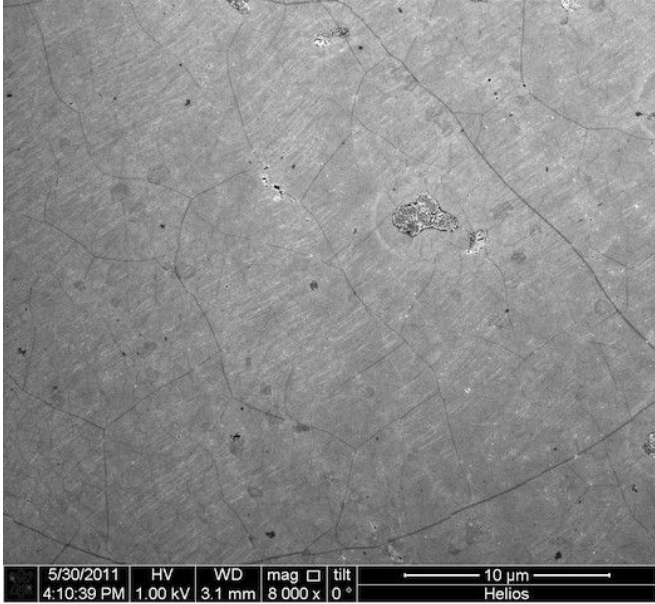


FIG. 1: Microphotograph of the graphene monolayer specimen

group. Fig. 2a shows the RS in initial sample "0" and sample 1 which was not irradiated. Initial sample "0" has a typical RS structure for monolayer graphene film⁷: there are three main lines in the spectrum: a weak D-line at 1350 cm^{-1} related to the inter-valley double resonant process in graphene with defects (edge, vacancy, etc.), a 2D-line at 2700 cm^{-1} , related to an inter-valley two phonon mode, characteristic for the perfect crystalline honeycomb structure, and a graphite-like G-line at 1600 cm^{-1} which is common for different carbon-based films. Usually, the ratio I_D/I_G between D and G lines is used as a measure of disorder in graphene films. The ratio I_D/I_G for the sample "0" is 0.15. This means that the initial film has a not bad quality though not being a perfect. It looks natural for the large size polycrystalline films. The perfect films with RS without D-line are usually obtained in the case of graphene flakes of small size about $10\text{ }\mu\text{m}$ or less.

Measurements of RS spectra in sample 1 showed that the ratio I_D/I_G increases from 0.15 up to 1.8 (Fig. 2a). It means that EBL introduces disorder itself, even without ion irradiation. Usually, in the case of small flakes, EBL does not lead to an increase of disorder. The damaging effect of EBL in our case could be explained by the presence of border regions in the polycrystalline film. The boundary regions may have a reduced adhesion to the SiO_2 substrate and therefore could be damaged by lift-off process during EBL.

Irradiation leads to further increase of disorder. Fig. 2b shows the transformation of the RS spectra in samples 2-6 with increasing irradiation dose Φ . Up to $\Phi = 1 \times 10^{14}\text{ cm}^{-2}$, the amplitude of the "defect" D-line increases, while the "perfect" 2D-line quickly disappears; new "defect" lines appear: D'-line (1620 cm^{-1}) and (D+G)-line

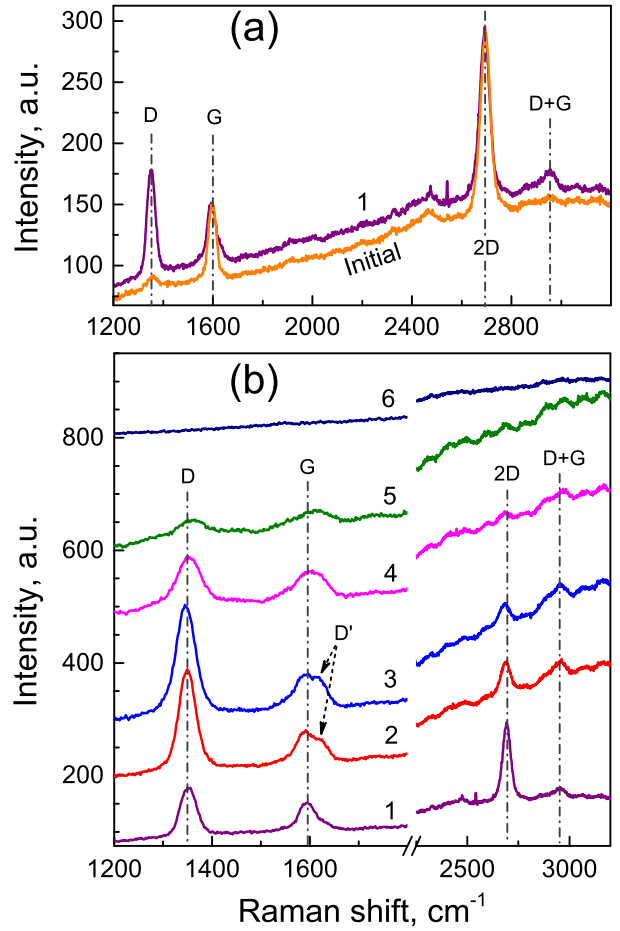


FIG. 2: (Color online) RS spectra: (a) - initial sample "0" and sample 1 (after EBL, non-irradiated); (b) - samples 1-6. $\Phi, \text{ cm}^{-2}$: 1- 0, 2 - 0.5×10^{14} , 3 - 1×10^{14} , 4 - 2×10^{14} , 5 - 4×10^{14} , 6 - 1×10^{15} . The lines are shifted for clarity

(2950 cm^{-1}). As to G-line, it remains approximately constant and only broadened because of appearance of the nearly located D'-line. So, intensity of D-line increases up to $I_D/I_G \approx 3.2$ at $\Phi = 10^{14}\text{ cm}^{-2}$. Further increase of the irradiation leads to decrease and broadening of D-line, so the ratio I_D/I_G decreases. On the latter stages, G-line also broadened, decreases and eventually, all RS structure disappears at $\Phi = 1 \times 10^{15}\text{ cm}^{-2}$ (sample 6). We are not aware about observation of complete disappearance of all RS lines in disordered graphene. Usually dependence of I_D/I_G as a function of disorder displays two different behaviors. In the regime of "low-defect-density", I_D/I_G increases with increase of the irradiation dose Φ . In the regime of "high-defect-density", I_D/I_G decreases with further increase of Φ , which is explained by amorphization of the graphen structure attenuating all Raman peaks. However, complete disappearance of all RS lines cannot be explained by amorphization, because G-line is observed even in amorphous carbon films¹². We assume that at the maximal level of disorder achieved in this experiment, the graphene film ceases to be a continu-

ous and splits into separate spots of small size (quantum dots). Small size of the quantum dots makes it impossible to form phonons responsible for the structural line of RS.

Degree of disorder can be characterized by the concentration of defects N_D (cm^{-2}) or by the mean distance between defects $L_D = N_D^{-1/2}$. Our irradiation conditions (C^+ ions with energy 35 keV) were the same as in Ref. 8 which were chosen such that the end-of-range damage would be away from the graphene film. In this case, concentration of induced defects N_D (vacancies, double vacancies, complex scattering centers, edges, etc.) is much less than the dose of irradiation Φ : $N_D = k\Phi$, where $k \ll 1$. Simulations showed that for our irradiation conditions, $k = 6 - 8\%$ ¹³.

We will use the empirical model which describes the dependence of I_D/I_G vs. L_D in both "low-defect-density" and "high-defect-density" regimes, that has been developed in Ref.¹⁴. In this model, a single defect causes modification of two length scale r_A and r_S ($r_A > r_S$). Just in the near vicinity of the defect, the area $S = \pi r_S^2$ is structurally disordered, but at $r_S < r < r_A$, the lattice structure is saved, though the proximity to a defect leads to breaking of selection rules and emission of D-line. The "activated" area responsible for D-line is $A = \pi(r_A^2 - r_S^2)$. In the "low-defect-density" regime, intensity of D-line linearly increases with N_D which means that $I_D/I_G \sim L_D^{-2}$ (the ratio I_D/I_G is used to normalize the intensity of D-line in comparison between different measurements). The maximal value of I_D is achieved when L_D decreases down to r_A ($L_D \approx r_A$). Further decrease of L_D leads to overlap between A-and S-areas which results in decrease of I_D/I_G . The rate equations which describes evolution of the S- and A-regions are

$$\frac{dS_S}{dN} = \pi r_S^2 \left(\frac{S_T - S_S}{S_T} \right) \quad (1)$$

$$\frac{dS_A}{dN} = \pi(r_A^2 - r_S^2) \left(\frac{S_T - S_S - S_A}{S_T} \right) - \pi r_S^2 \frac{S_A}{S_T}. \quad (2)$$

Here S_S , S_A and S_T denote the structurally disordered, activated and total areas of the film and N is the number of the induced defects. The last term in Eq. (2) describes the overlap of S- and A-areas, which was omitted in¹⁴. With this term, the final equation for the dependence $I_D/I_G(L_D)$ has the form:

$$I_D/I_G = C_A e^{-\pi r_S^2/L_D^2} \left[1 - e^{-\pi(r_A^2 - r_S^2)/L_D^2} \right] + C_S \left[1 - e^{-\pi r_S^2/L_D^2} \right]. \quad (3)$$

Actually, Eq. (3) could be obtained directly from basic probability theory, taking into account that for the Poisson distribution of the defect positions the quantity $e^{-\pi r_S^2/L_D^2}$ is just the probability that there are no defects in the circle with radius r_S . Thus the multiplier $1 - e^{-\pi r_S^2/L_D^2}$ gives the fraction of the structurally-disorder region; similarly the multiplier

$e^{-\pi r_S^2/L_D^2} \left[1 - e^{-\pi(r_A^2 - r_S^2)/L_D^2} \right]$ gives the fraction of the activated region.

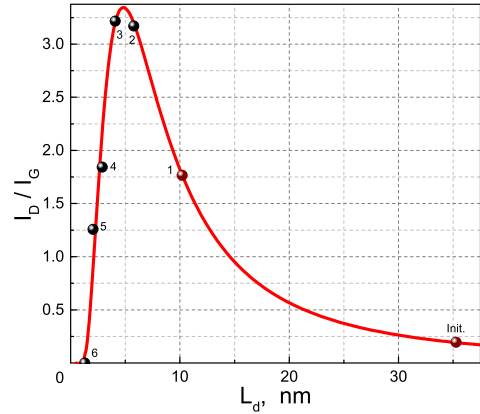


FIG. 3: Ratio I_D/I_G as a function of the mean distance between defects L_D . Solid line represents Eq.(3) with $C_A = 5.4$, $C_S = 0$, $r_S = 1.55$ nm, $r_A = 4.1$ nm.

Fig. 3 shows the result of fitting the theoretical curve (Eq.(3)) with experimental data. First, the experimental points for irradiated samples 2-6 were plotted. We choose $k = 6\%$; L_D for these samples was defined as $L_D = (0.06\Phi)^{-1/2}$. Then, the curve (Eq.(3)) was fitted to the experimental points. Finally, the values of I_D/I_G for non-irradiated samples "0" and 1 were placed "by hand" on the curve. This allows to estimate L_D for these samples and, therefore, the density of defects N_D in initial film as $8 \times 10^{10} \text{ cm}^{-2}$ and in sample 1 as $1 \times 10^{12} \text{ cm}^{-2}$. As a result, we can plot the RS data for all samples on the scale I_D/I_G as a function of N_D . This dependence is shown in Fig. 4.

IV. SAMPLE RESISTANCE

In Fig. 4, the resistance R at room temperature for all samples is also shown. Resistance of "initial" sample "0", is $R \approx 600$ Ohm, which agrees with the numerous data reported for the resistivity of pristine graphene (in our samples, resistivity is equal to resistance due to square geometry). One can see that increase of N_D leads to the strong continuous increase of R over many orders of magnitude. Fig. 4 demonstrate also a relationship between structure and resistance of disordered graphene. Maximum value of the ratio I_D/I_G occurs at $N_D \approx 4 \times 10^{12} \text{ cm}^{-2}$, when L_D (5 nm) is indeed close to r_A (4.1 nm). In other words, at this N_D , the "activated" A-area fills all the sample space. Fig. 4 shows also, that the maximum I_D/I_G corresponds to the film resistance $R_{max} \approx 20$ kOhm, which is approximately equal to the reciprocal value of the minimal conductivity in graphene $4e^2/\pi h$ (see e.g. Ref. 15) or to the resistance quantum $h/e^2 \approx 25.8$ kOhm. This allows us to conclude that the graphene film with $R \gg R_{max}$ is not continuous

which supports the assumption about fragmentation of the highly disordered graphene film which was made on the basis of disappearance of the RS lines.

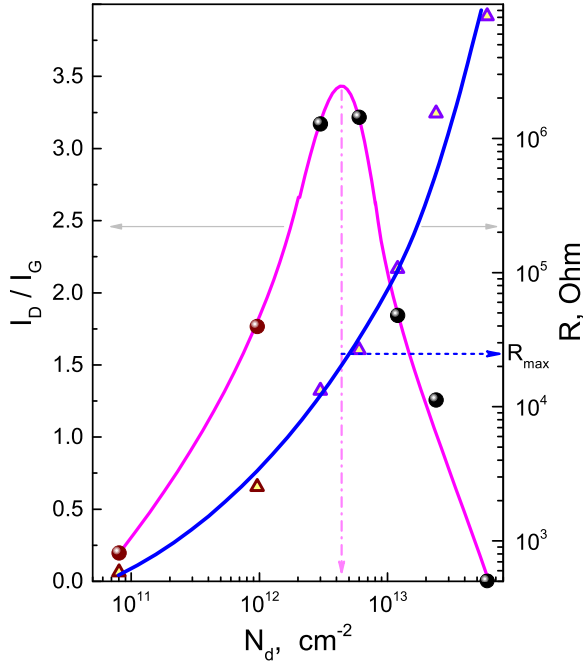


FIG. 4: The RS line ratio I_D/I_G and the sample resistance R at 300 K plotted as a function of the defect concentration N_D .

Measurements of the current-voltage characteristics ($I - V$) showed that for weakly disordered films (samples 1 - 4), $I - V$ characteristics is linear (Ohmic regime), while for highly disordered films (samples 5 and 6), $I - V$ is strongly non-linear. Fig. 5 shows the static resistance $R = V/I$ as a function of the current for samples 2 - 6. For samples 5 and 6, R has the maximal value R_0 at $I \rightarrow 0$ and falls with increase of I or V . The values of R_0 are plotted for samples 5 and 6 in Fig. 4. The change in the character of $I - V$ for highly irradiated samples can

be explained by the replacement of usual conductivity along the continuous film by the field-induced electron tunneling between quantum dots.

We conclude with the statement that at the ultimate stage of disorder induced by ion irradiation, the graphene film ceases to be continuous and is fragmented to separated small-size graphene islands (quantum dots). Fragmentation of graphene film is accompanied by complete disappearance of the Raman spectra lines and change in the $I - V$ characteristics which reflects the different mechanism of conductivity. The maximal resistance of the continuous disordered graphene film is of order of

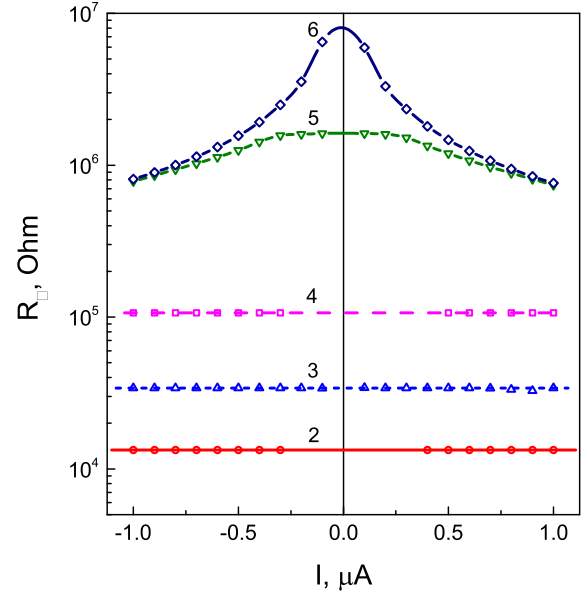


FIG. 5: Static resistance $R = V/I$ as a function of current I for samples 2 - 6.

reciprocal value of the minimal graphene conductivity.

* Electronic address: Issai.Shlimak@biu.ac.il

¹ M. I. Katsnelson, *Graphene: Carbon in Two Dimensions*, (Cambridge University Press, 2012).

² L. E. F. Foa Torres, S. Roche, J.-C. Charlier, *Introduction to Graphene-Based Nanomaterials: From Electronic Structure to Quantum Transport*, (Cambridge University Press, 2014).

³ J. H. Warner, F. Schaffel, M. Rummeli, A. Bachmatiuk, *Graphene: Fundamentals and emergent applications*, (El-

sevier, 2012).

⁴ L. Liu, S. Ryu, M. R. Tomasik, E. Stolyarova, N. Jung, M. S. Hybertsen, M. L. Steigerwald, L. E. Brus, G. W. Flynn, *Nano Lett.* **8**, 1965 (2008).

⁵ D. C. Elias, R. R. Nair¹, T. M. G. Mohiuddin¹, S. V. Morozov, P. Blake, M. P. Halsall, A. C. Ferrari⁴, D. W. Boukhvalov, M. I. Katsnelson, A. K. Geim, K. S. Novoselov, *Science* **323**, 610 (2009).

⁶ H. Liu, Y. Liu, and D. Zhua, *J. Mater. Chem.* **21**, 3335

⁷ (2011).

⁷ R. Saito, M. Hofmann, G. Dresselhaus, A. Jorio, M.S. Dresselhaus, *Adv. Phys.* **30**, 413 (2011).

⁸ G. Buchowicz, P.R. Stone, J.T. Robinson, C.D. Cress, J.W. Beeman, O.D. Dubon, *Appl. Phys. Lett.* **98**, 032102 (2011).

⁹ B. Guo, Q. Liu, E. Chen, H. Zhu, L. Fang, J.R. Gong, *NanoLett.* **10**, 4975 (2010).

¹⁰ Q. Wang, W. Mao, D. Ge, Y. Zhang, Y. Shao, N. Ren, *Appl. Phys. Lett.* **103**, 073501 (2013).

¹¹ A.C. Ferrari, J.C. Meyer, V. Scardaci, C. Casiraghi, M. Lazzeri, F. Mauri, S. Piscanec, D. Jiang, K.S. Novoselov, S. Roth, and A.K. Geim, *Phys. Rev. Lett.* **97**, 187401 (2006).

¹² A. C. Ferrari and J. Robertson, *Phys. Rev. B* **61**, 14 095 (2000).

¹³ O. Lehtinen, J. Kotakoski, A.V. Krasheninnikov, A. Tolvanen, K. Nordlund, and J. Keinonen, *Phys. Rev. B* **81**, 153401 (2010).

¹⁴ M.M. Lucchese, F. Stavale, E.H. Ferreira, C. Vilani, M.V.O. Moutinho, R.B. Capaz, C.A. Achete, and A. Jorio, *Carbon* **48**, 1592 (2010).

¹⁵ K. Ziegler, *Phys. Rev. Lett.* **97**, 266802 (2006).